

Article

Implications of W-Boson Mass Anomaly for Atomic Parity Violation

Hoang Bao Tran Tan * and Andrei Derevianko 

Department of Physics, University of Nevada, Reno, NV 89557, USA

* Correspondence: htrantan@unr.edu

Abstract: We consider the implications of the recent measurement of the W-boson mass $M_W = 80,433.5 \pm 9.4 \text{ MeV}/c^2$ for atomic parity violation experiments. We show that the change in M_W shifts the Standard Model prediction for the ^{133}Cs nuclear weak charge to $Q_W(^{133}\text{Cs}) = -73.11(1)$, i.e., by 8.5σ from its current value, and the proton weak charge by 2.7%. The shift in $Q_W(^{133}\text{Cs})$ ameliorates the tension between existing determinations of its value and motivates more accurate atomic theory calculations, while the shift in $Q_W(p)$ inspires next-generation atomic parity violation experiments with hydrogen. Using our revised value for $Q_W(^{133}\text{Cs})$, we also readjust constraints on parameters of physics beyond the Standard Model. Finally, we reexamine the running of the electroweak coupling for the new W boson mass.

Keywords: W-boson mass anomaly; atomic parity violation; physics beyond the standard model

1. Introduction

Atomic parity violation (APV) is a major means for testing the electroweak (EW) sector of the Standard Model (SM) at low energy. Currently, the best APV result provides a confirmation of the SM prediction of the ^{133}Cs nuclear weak charge at the level of 0.35% accuracy [1]. Future APV experiments with expected accuracy 0.1–0.2% [2–9] may help resolve the tension between high-energy Z-pole measurements of $\sin^2 \theta_W$ (here θ_W is the weak mixing angle) [10,11] when extrapolated to the APV scale. APV experiments are also uniquely sensitive to a certain class of new physics to which high-energy probes are blind.

The use of APV to constrain physics beyond the SM relies on precise measurement of the APV amplitude E_{PV} , accurate theoretical calculation of the atomic structure factor k_{PV} needed for extracting the nuclear weak charge Q_W via $E_{PV} = k_{PV}Q_W$, and exact knowledge of the SM prediction for Q_W against which the experimentally extracted value is compared. The most accurate measurement of E_{PV} comes from the Boulder group for ^{133}Cs with an uncertainty of 0.35% [1], although a new experiment is being planned with an aim of a 0.2% accuracy [4,5].

Early atomic calculations of k_{PV} for ^{133}Cs at the level of 0.4% uncertainty [12–15] gave a value of Q_W that is 2.5σ away from the SM prediction. Later developments resulted in the inclusion of sub-1% contributions from Breit and QED corrections and culminated in the most detailed coupled-cluster singles doubles and valence triples calculation (CCSDvT) with an uncertainty of 0.27% and a value for Q_W in an essential agreement with the SM [16]. A more recent reevaluation yielded a Q_W , which is 1.5σ away from the SM value whilst raising the theoretical uncertainty back to 0.5% [17]. The latest 0.3%-accurate calculation [18–20] gives a result agreeing with Ref. [16]. A new parity-mixed coupled-cluster approach to calculating k_{PV} is under development [21], with a goal of reducing the theoretical uncertainty to 0.2%.

Once the values of E_{PV} and k_{PV} are known, the nuclear weak charge Q_W may be extracted using $E_{PV} = k_{PV}Q_W$ and compared with the SM prediction. A disagreement between the two results could provide hints about physics beyond the SM. Within the SM



Citation: Tran Tan, H.B.; Derevianko, A. Implications of W-Boson Mass Anomaly for Atomic Parity Violation. *Atoms* **2022**, *10*, 149. <https://doi.org/10.3390/atoms10040149>

Academic Editors: Ulrich D. Jentschura and Alexander Kramida

Received: 15 November 2022

Accepted: 7 December 2022

Published: 9 December 2022

Publisher's Note: MDPI stays neutral with regard to jurisdictional claims in published maps and institutional affiliations.



Copyright: © 2022 by the authors. Licensee MDPI, Basel, Switzerland. This article is an open access article distributed under the terms and conditions of the Creative Commons Attribution (CC BY) license (<https://creativecommons.org/licenses/by/4.0/>).

itself, Q_W is expressed in terms of the axial–electron–vector–nucleon coupling constants g_{AV}^{ep} and g_{AV}^{en} . At the tree level, these coupling constants depend on the weak mixing angle, with one-loop and leading two-loop corrections coming from the W and Z boson self-energies, the γZ mixing renormalization of $\sin^2 \theta_W$, and the so-called WW , ZZ , and γZ box diagrams [22–25]. The low-energy value of $\sin^2 \theta_W$ may be obtained from the measured Z -pole value by using its scale dependence. New physics contributions to the weak charge Q_W may arise from multiple mechanisms: (i) tree-level exchange of a new Z' boson with mass at the TeV scale [26,27], (ii) corrections to the W and Z boson self-energies due to vacuum polarization involving beyond-SM particles [26,28], (iii) kinetic and mass mixing of a “dark” Z_d boson of mass $\sim \text{MeV} - \text{GeV}$ with the photon and the Z boson [29–31], or (iv) an oscillating $\bar{\theta}_{\text{QCD}}$ term in the form of interaction with the axion and axion-like particles [32].

The reference SM value for the weak mixing angle is usually obtained from global fits of electroweak observables such as masses and widths of the Z and W bosons as well as left-right and forward-backward asymmetries in a variety of scattering processes involving the weak interaction. In this paper, we focus on the implications of the recently reported W boson mass from the CDF II collaboration, which shows a 7σ deviation from the current global fit value [33]. We show that the CDF II stand-alone result implies a shift in the Z -pole value of the weak mixing angle and thereby modifies the SM value of the ^{133}Cs nuclear weak charge Q_W . Similarly, it shifts the value of the proton weak charge by 2.7%, further motivating APV experiments in hydrogen. By using the new value of $Q_W^{\text{SM}}(^{133}\text{Cs})$ implied by the W boson mass anomaly [33] and existing APV results for ^{133}Cs , we readjust limits on the ratio of the coupling-to-mass of the new Z' boson, the weak isospin-conserving parameter of vacuum polarization effects on gauge boson propagators, and on the parameters describing the SM couplings to a dark Z_d boson. Implications of the new W boson mass measurement [33] for other physics beyond the SM scenarios were considered in Refs. [34–43].

2. Theory

2.1. Electroweak Phenomenology and Atomic Parity Violation

The electroweak (EW) sector of the standard model is described in terms of the $SU(2)_L \times U(1)_Y$ gauge group with corresponding vector fields W_μ^i ($i = 1, 2, 3$) and B_μ with gauge couplings g and g' (see, e.g., Refs. [44,45]). Spontaneous breaking of the EW gauge symmetry is effected by introducing a complex scalar Higgs doublet ϕ with a Lagrangian

$$\mathcal{L}_\phi = (D_\mu \phi)^\dagger (D^\mu \phi) + \mu^2 \phi^\dagger \phi + \frac{\lambda^2}{2} (\phi^\dagger \phi)^2, \tag{1}$$

where the covariant derivative is defined as

$$D_\mu \phi \equiv \left(\partial_\mu + \frac{ig}{2} \sigma_i W_\mu^i + \frac{ig'}{2} B_\mu \right) \phi. \tag{2}$$

Here, σ_i are the Pauli matrices.

For $\mu^2 < 0$, the potential (1) has a minimum at $v = \sqrt{2}|\mu|/\lambda$, around which point ϕ may be transformed into a single real scalar field H with vanishing vacuum expectation value. After such a transformation, one finds that the Lagrangian (1) contains the following terms

$$\mathcal{L}_\phi \supset \frac{1}{2} M_H^2 H^2 + M_W^2 W^{\mu-} W_\mu^+ + \frac{1}{2} M_Z^2 Z^\mu Z_\mu, \tag{3}$$

where

$$W_\mu^\pm \equiv \frac{W_\mu^1 \pm iW_\mu^2}{\sqrt{2}}, \tag{4}$$

$$Z_\mu \equiv \frac{gW_\mu^3 - g'B_\mu}{\sqrt{g^2 + g'^2}}, \tag{5}$$

are the charged W boson and neutral Z boson fields, and

$$M_H = \lambda v, \tag{6}$$

$$M_W = gv/2, \tag{7}$$

$$M_Z = \sqrt{g^2 + g'^2}v/2, \tag{8}$$

are the masses of the Higgs boson, W boson, and Z boson, respectively.

The Higgs field breaks the $SU(2)_L \times U(1)_Y$ symmetry down to an $SU(2)_{\text{weak}}$ symmetry of weak interactions mediated by the W^\pm and Z bosons (see Equations (4)) and a $U(1)_{\text{elec}}$ symmetry with electromagnetic interactions mediated by the photon field $A_\mu \equiv \frac{gW_\mu^3 - g'B_\mu}{\sqrt{g^2 + g'^2}}$. With this, the Lagrangian for the fermion fields ψ_i reads

$$\mathcal{L}_F = \sum_i \bar{\psi}_i \left[i\partial - m_i \left(1 + \frac{H}{v} \right) \right] \psi_i - \frac{g}{\sqrt{2}} \left(J_W^{\mu+} W_\mu^+ + J_W^{\mu-} W_\mu^- + J_A^\mu A_\mu + J_Z^\mu Z_\mu \right), \tag{9}$$

where m_i is the fermion mass and $\partial \equiv \gamma^\mu \partial_\mu$. The definitions for the weak charged current J_W^μ , the weak neutral current J_Z^μ , and the electromagnetic current J_A^μ may be found, e.g., in Ref. [46]. For small momentum transfer $Q^2 \ll M_{W,Z}^2$, the interaction terms in Equation (9) reduce to the effective charged (\mathcal{L}_{CC}) and neutral current (\mathcal{L}_{NC}) interactions

$$\mathcal{L}_{CC} = -2J_W^{\mu+} J_{W\mu} / v^2, \tag{10}$$

$$\mathcal{L}_{NC} = -\cos^2 \theta_W J_Z^\mu J_{Z\mu} / v^2, \tag{11}$$

where $G_F \equiv 1/(\sqrt{2}v^2) = g^2/(2\sqrt{2}M_W^2)$ is the Fermi constant and $\theta_W = \tan^{-1}(g'/g)$ is the Weinberg angle. The effective four-fermion interaction (11) contains a parity-violating (PV) interaction

$$\mathcal{L}_{NC}^{eq} = \frac{G_F}{\sqrt{2}} \bar{e} \gamma_\mu \gamma_5 e \left(g_{AV}^{eu} \bar{u} \gamma^\mu u + g_{AV}^{ed} \bar{d} \gamma^\mu d \right), \tag{12}$$

describing the couplings between electrons and quarks by exchange of a Z boson. Here, g_{AV}^{eu} and g_{AV}^{ed} are the axial–electron–vector–quark coupling constants, related to the axial–electron–vector–nucleon coupling constants via $g_{AV}^{ep} = 2g_{AV}^{eu} + g_{AV}^{ed}$ and $g_{AV}^{en} = g_{AV}^{eu} + 2g_{AV}^{ed}$. It is this interaction that ultimately gives rise to the spin-independent APV observables. For a more comprehensive review of low-energy EW experiments, see, e.g., Ref. [47].

The EW Lagrangians (1) and (9) depend on the set of parameters $\{g, g', \mu^2, \lambda^2, m_i\}$, whose values cannot be derived algebraically from within the SM and can only be determined experimentally. For this purpose, it may be more convenient to measure other sets of derived quantities, such as $\{g, \theta_W, M_H, v, m_i\}$ or $\{M_Z, \alpha, M_W, G_F, m_i\}$, where $\alpha = e^2/(\hbar c)$ is the fine-structure constant. Among these derived parameters, the quantities M_Z , G_F , and α have the lowest experimental errors. Namely, $M_Z = 91.1876(21)$ GeV was determined from the Z line-shape scan [48], $G_F = 1.1663787(6) \times 10^{-5}$ GeV⁻² was derived from muon lifetime [49], and $\alpha = 1/137.035999084(21)$ was obtained by combining measurements of the e^\pm anomalous magnetic moment [50] with measurements of the Rydberg constant and atomic masses with interferometry of atomic recoil kinematics [51,52]. As a result, we keep these fixed in our analysis below.

The quantities θ_W , M_W , M_H , and m_t are generally less well constrained (except for $m_{e,\mu,\tau}$). The Weinberg angle θ_W , or more precisely, $\sin^2 \theta_W$, is measured in a variety of schemes, depending on the energy scale, including low-energy APV [1,53–62], PV neutrino scattering [63–66], as well as various types of asymmetries in scattering and decay processes at low energy [67–75] and high energy [10,48,76–81]. The mass M_W is obtained in W -pair production or single- W production at energy $Q \sim M_Z$ [76–78]. Combining $\sin^2 \theta_W$ and M_W allows one to constrain M_H and the top quark mass m_t via [82].

$$M_W^2 \sin^2 \theta_W = \frac{A^2}{1 - \Delta r}, \tag{13}$$

where $A \equiv \sqrt{\pi\alpha/(\sqrt{2}G_F)}$ and Δr includes loop corrections to M_W , which depend on m_t and M_H . Alternatively, one may use direct experimental values for m_t and M_H to constrain M_W and $\sin^2 \theta_W$.

We note that there exist in the literature several different definitions for $\sin^2 \theta_W$. At the tree level, one has

$$\sin^2 \theta_W = 1 - \frac{M_W^2}{M_Z^2} = \frac{g'^2}{g^2 + g'^2}. \tag{14}$$

One may promote the first equality in Equation (14) to a definition of the renormalized $\sin^2 \theta_W$ to all orders in perturbation theory (the so-called on-shell scheme). In this case, the radiative correction Δr has a quadratic dependence on m_t ,

$$\Delta r \approx 1 - \frac{\alpha}{\hat{\alpha}_Z} - \frac{3G_F m_t^2 \cos^2 \theta_W}{8\sqrt{2}\pi^2 \sin^2 \theta_W} + \frac{11\alpha}{48\pi \sin^2 \theta_W} \ln \frac{M_H^2}{M_Z^2}, \tag{15}$$

where $\hat{\alpha}_Z \equiv \alpha(M_Z)$ is the value of the fine structure constant at M_Z and may receive large spurious contributions from higher orders $O(\alpha m_t^2/M_W^2)$. A more popular approach promotes the second equality in Equation (14) to an $\overline{\text{MS}}$ (modified minimal subtraction) prescription with the quantity

$$\sin^2 \hat{\theta}_W(\mu) \equiv \frac{\hat{g}'^2(\mu)}{\hat{g}^2(\mu) + \hat{g}'^2(\mu)}, \tag{16}$$

where \hat{g}' and \hat{g} are $\overline{\text{MS}}$ quantities, and μ is an energy scale conventionally chosen to be M_Z . With this $\overline{\text{MS}}$ definition, the identity (13) becomes

$$M_W^2 \sin^2 \hat{\theta}_W = \frac{A^2}{1 - \Delta \hat{r}_W}, \tag{17}$$

where the radiative correction $\Delta \hat{r}_W$ now has no quadratic dependence on m_t ,

$$\Delta \hat{r}_W \approx 1 - \frac{\alpha}{\hat{\alpha}_Z} + \frac{4\alpha}{48\pi\hat{s}_Z^2} \ln \frac{M_H^2}{M_Z^2}, \tag{18}$$

where $\hat{s}_Z^2 \equiv \sin^2 \hat{\theta}_W(M_Z)$. The $\overline{\text{MS}}$ and on-shell definitions are related via

$$\hat{s}_Z^2 = c(m_t, M_H) \sin^2 \theta_W, \tag{19}$$

with a multiplicative coefficient $c(m_t, M_H) = 1.0351(3)$ [82]. For APV, the quantity

$$\hat{s}_0^2 \equiv \sin^2 \hat{\theta}_W(0)$$

is relevant, where the energy scale is set to zero.

Let us now consider the EW phenomenology at low energies. In particular, we concentrate on APV parameterized by a nuclear weak charge Q_W . The nuclear weak charge

Q_W arises as a parameter of the effective APV Hamiltonian density obtained by integrating out the quark fields in the Lagrangian density (12), obtaining

$$\mathcal{L}_{\text{NC}}^{eq} \rightarrow H_W = -\frac{G_F}{2\sqrt{2}} \bar{e}(\mathbf{r}) \gamma_5 e(\mathbf{r}) Q_W \rho(\mathbf{r}), \tag{20}$$

where $\rho(r)$ is the nuclear density. The nuclear weak charge Q_W receives coherent contributions from both protons and neutrons and may be written, at the tree level, as [82].

$$Q_W = Z(1 - 4\hat{s}_0^2) - N, \tag{21}$$

where Z is the atomic number, and N is the number of neutrons. Here, we have assumed that $\sin^2 \hat{\theta}_W$ evaluated at the relevant APV momentum transfer of $Q \approx 2.4$ MeV is, to good accuracy, the same as \hat{s}_0^2 ; see Ref. [83] for further details. Radiative corrections to Equation (21) come from the W and Z boson self-energies, the γZ mixing renormalization of $\sin^2 \theta_W$, and the so-called WW , ZZ , and γZ box diagrams [22–25] also depend on M_W , either directly $\sim \ln M_W^2$ or indirectly via the value of the strong coupling constant evaluated at M_W .

The interaction (20) mixes atomic states with opposite parities and thus gives rise to the otherwise forbidden electric-dipole transitions between two states with the same nominal parity, e.g., $6S_{1/2} \rightarrow 7S_{1/2}$ in ^{133}Cs . A measurement of the amplitude of such a transition leads to the extraction of the values Q_W and \hat{s}_0^2 , which may then be compared with the SM predictions to give hints about new physics. In the next section, we present several mechanisms through which new physics effects may alter the SM value for the nuclear weak charge Q_W .

2.2. New Physics Contributions to Atomic Parity Violation

In this section, we consider three beyond-SM contributions to the nuclear weak charge Q_W , namely, a tree-level exchange of a new Z' boson, corrections to the Z and W boson self-energies through quantum loops involving beyond-SM particles, and SM particles coupling to a new dark Z_d boson. Although the results presented here are not new, they serve as a basis for our discussions in Section 4.

Let us begin with the tree-level correction due to the exchange of a new heavy Z' boson, which appears in several extensions of the SM, including $SO(10)$, E_6 , and extradimensional theories [84–91]. In the low energy limit, this yields an additional term similar to the effective Lagrangian (12).

$$\mathcal{L}_{\text{NC}}^{leq} = \frac{1}{M_{Z'}^2} \bar{e} \gamma_\mu \gamma_5 e \left(f_{AV}^{eu} \bar{u} \gamma^\mu u + f_{AV}^{ed} \bar{d} \gamma^\mu d \right), \tag{22}$$

where f_{AV}^{eu} and f_{AV}^{ed} are the axial-electron-vector-quark coupling constants for the exchange of the new Z' boson of mass $M_{Z'}$ [92,93]. By integrating out the quark degrees of freedom, we obtain the following contribution to Q_W

$$\Delta Q_W^{Z'} = -\frac{2\sqrt{2}}{G_F} \frac{\bar{f}_{AV}^{eq}}{M_{Z'}^2} 3(Z + N), \tag{23}$$

where the average electron-quark coupling \bar{f}_{AV}^{eq} is defined as

$$\bar{f}_{AV}^{eq} = \frac{f_{AV}^{eu}(2Z + N) + f_{AV}^{ed}(Z + 2N)}{3(Z + N)}. \tag{24}$$

In a simple model where Z' has the same couplings as Z , Equation (23) reduces to [26,27,94]

$$\Delta Q_W^{Z'} = -Q_W^{SM} \frac{M_Z^2}{M_{Z'}^2}. \tag{25}$$

We note that the analysis above applies only to the case where the mass of the new Z' boson is much larger than the relevant momentum transfer ($Q \approx 2.4$ MeV in the case of APV in ^{133}Cs). If, on the other hand, $M_{Z'} \ll Q$, then the local approximation for the Z' boson propagator leading to the contact interaction (22) is no longer valid. Instead, the exchange of a light Z' boson gives rise to a (long range) Yukawa-like PV interaction [92,93].

$$\Delta H'_W = -\frac{G_F}{2\sqrt{2}} \bar{e}(\mathbf{r}) \gamma_5 e(\mathbf{r}) \Delta Q_W \frac{M_{Z'}^2}{4\pi r} e^{-M_{Z'} r} \rho(\mathbf{r}). \tag{26}$$

The effect of this on Q_W is equivalent to multiplying Equation (23) by a factor

$$K(M_{Z'}) = \frac{\int \langle \bar{e}(\mathbf{r}) \gamma_5 e(\mathbf{r}) \rangle \frac{M_{Z'}^2 e^{-M_{Z'} r'}}{4\pi r'} \rho(\mathbf{r}') d^3 r d^3 r'}{\langle \bar{e}(\mathbf{r}) \gamma_5 e(\mathbf{r}) \rangle \rho(\mathbf{r}') d^3 r d^3 r'}, \tag{27}$$

which accounts for the long range nature of the interaction. For $M_{Z'} \approx 2.4$ MeV, $K(M_{Z'}) = 1/2$.

Next, we consider vacuum polarization effects of the self-energies $\Pi_{WW}(q^2)$ and $\Pi_{ZZ}(q^2)$ of the W and Z bosons. These effects may arise, for example, from quantum loops involving supersymmetric [95] or technicolor particles [96]. The form of Equation (17) is especially convenient for including these contributions. Regardless of their nature, if the new physics phenomena are associated with very large energy scales, their effects at low energies may be described solely by the weak isospin-conserving parameters S_W and S_Z and the weak isospin-breaking parameters T defined by [26,28,97].

$$\frac{\Pi_{WW}^{\text{new}}(0)}{M_W^2} - \frac{\Pi_{ZZ}^{\text{new}}(0)}{M_Z^2} = \alpha(M_Z) T, \tag{28}$$

$$\left[\frac{\Pi_{WW}^{\text{new}}(M_W^2) - \Pi_{WW}^{\text{new}}(0)}{M_W^2} \right]_{\text{MS}} = \frac{\alpha(M_Z)}{4\hat{s}_0^2} S_W, \tag{29}$$

$$\left[\frac{\Pi_{ZZ}^{\text{new}}(M_Z^2) - \Pi_{ZZ}^{\text{new}}(0)}{M_Z^2} \right]_{\text{MS}} = \frac{\alpha(M_Z)}{4\hat{s}_0^2(1 - \hat{s}_0^2)} S_Z, \tag{30}$$

where Π_{WW}^{new} and Π_{ZZ}^{new} are new physics vacuum polarization contributions, and $\alpha(M_Z) \approx 1/127.94$ is the fine-structure constant at M_Z .

To the leading order, the new physics effects modify the ^{133}Cs weak charge by contributing to the radiative corrections to G_F and \hat{s}_0^2 . The contribution to G_F may be conveniently expressed via a multiplicative factor, $G_F \rightarrow \rho^{\text{new}} G_F$, where

$$\rho^{\text{new}} = 1 + \frac{\Pi_{WW}^{\text{new}}(0)}{M_W^2} - \frac{\Pi_{ZZ}^{\text{new}}(0)}{M_Z^2} = 1 + \alpha(M_Z) T \approx 1 + 0.00782 T, \tag{31}$$

by virtue of Equation (28). Assuming that $S_W = S_Z = S$, the quantity $\Delta \hat{r}_W$ in Equation (17) receives an additional contribution [26].

$$\Delta \hat{r}_W^{\text{new}} = \left[\frac{\Pi_{ZZ}^{\text{new}}(M_Z^2) - \Pi_{WW}^{\text{new}}(0)}{M_W^2} \right]_{\text{MS}} = \frac{\alpha(M_Z)}{4\hat{s}_0^2(1 - \hat{s}_0^2)} S - \alpha(M_Z) T, \tag{32}$$

which, when solved for \hat{s}_0^2 perturbatively, gives

$$(\Delta \hat{s}_0^{\text{new}})^2 = 0.00365 S - 0.00261 T. \tag{33}$$

By using Equations (31) and (33) in Equation (21), one finds the beyond-SM contribution the ^{133}Cs weak charge as [98].

$$\Delta Q_W^{ST} (^{133}\text{Cs}) = -0.800S - 0.007T. \tag{34}$$

where the suppression of the T -contribution is a result of an accidental cancellation between ρ^{new} and $\Delta \hat{\rho}_W^{\text{new}}$ particular to ^{133}Cs . Equation (34) shows that the ^{133}Cs APV experiment is sensitive to S but not T .

Finally, we consider the effects of a dark Z_d boson of mass $M_{Z_d} \sim \text{MeV-GeV}$, which couples to the SM via kinetic mixing with the photon and mass mixing with the Z boson. Such a particle arises from an extra $U(1)_d$ gauge symmetry and is a prominent dark matter candidate (the dark photon) [99–102]. The extended QED Lagrangian with the new $U(1)_d$ included reads [103].

$$\mathcal{L}_{Z_d} = -\frac{Z_d^{\mu\nu} Z_{d\mu\nu}}{4} - M_{Z_d}^2 Z_d^\mu Z_{d\mu} + \frac{\epsilon B_{\mu\nu} Z_d^{\mu\nu}}{2 \cos \theta_W}, \tag{35}$$

where $B_{\mu\nu} = \partial_\mu B_\nu - \partial_\nu B_\mu$ and $Z_{d\mu\nu} = \partial_\mu Z_{d\nu} - \partial_\nu Z_{d\mu}$ are the field strengths for the $U(1)_Y$ and $U(1)_d$ vector fields, respectively. The kinetic mixing term in Equation (35) may be removed by shifting $B_\mu \rightarrow B_\mu + \frac{\epsilon}{\cos \theta_W} Z_{d\mu}$, with which the photon and Z boson fields become $A_\mu \rightarrow A_\mu + \epsilon Z_{d\mu}$ and $Z_\mu \rightarrow Z_\mu - \epsilon \tan \theta_W Z_{d\mu}$. As a result of this field redefinition, an induced coupling of Z_d to the SM electromagnetic current J_{em}^μ appears and has the form

$$\mathcal{L}_{\text{em}}^{Z_d} = -e\epsilon J_{\text{em}}^\mu Z_{d\mu}. \tag{36}$$

Neutral-current couplings of Z_d to the SM sector may be included by introducing a $Z - Z_d$ mass mixing

$$\mathcal{L}_{\text{mass mixing}} = -\epsilon_Z M_Z^2 Z^\mu Z_{d\mu}, \tag{37}$$

with a mixing coefficient $\epsilon_Z = (M_{Z_d} / M_Z)\delta$, where δ is a small model-dependent quantity [30,104]. The vacuum oscillations between the Z and Z_d fields due to mass mixing may be removed by another field redefinition, after which Z_d couples directly to the SM sector via

$$\mathcal{L}_{\text{NC}}^{Z_d} = -\frac{g\epsilon_Z}{\cos \theta_W} J_Z^\mu Z_{d\mu}, \tag{38}$$

where J_Z^μ is again the weak neutral current appearing in Equation (9).

Both interactions (36) and (38) contribute to parity violation due to electron-quark coupling by exchanging a Z_d boson. As with the exchange of a Z boson, the electron vertex is the axial part of Equation (38). The quark vertex, on the other hand, can either be the vector part of Equation (38) (as with a Z boson) or the electromagnetic coupling (36). The overall effect of the interactions (36) and (38) for APV thus appears as a modification of the nuclear weak charge (assuming that M_{Z_d} is much larger than the momentum exchange) [30,104]

$$\Delta Q_W^{Z_d} = \delta^2 Q_W^{SM} + 4Z \frac{\epsilon}{\epsilon_Z} \delta^2 \cos \hat{\theta}_W \sin \hat{\theta}_W. \tag{39}$$

The quantities $\hat{f}_{AV}^{eq} / M_{Z'}^2$, S , δ and ϵ / ϵ_Z parameterizing the new physics contributions to APV have been constrained by comparing the measured values of $Q_W(^{133}\text{Cs})$ with the SM prediction. In the next section, we consider the recent result from the CDF II Collaboration for M_W which shows a significant 7σ tension with the SM [33]. We shall assume that all other quantities except $\sin^2 \hat{\theta}_W$ remain the same. By the virtue of Equation (17), the shift in M_W then implies a corresponding change in the value of $\sin^2 \hat{\theta}_W(M_Z)$ and thus of $Q_W(^{133}\text{Cs})$ via \hat{s}_0^2 . We will use this “new” SM value for $Q_W(^{133}\text{Cs})$ to adjust existing constraints on $\hat{f}_{AV}^{eq} / M_{Z'}^2$, S , δ and ϵ / ϵ_Z .

3. Numerical Results

The value of \hat{s}_0^2 as predicted by the SM may be related to the W boson mass M_W via Equation (17) and the running of the weak angle [24,105,106].

$$\sin^2 \hat{\theta}_W(Q^2) = \kappa(Q^2) \sin^2 \hat{\theta}_W(M_Z) = \frac{\kappa(Q^2) A^2}{M_W^2 (1 - \Delta \hat{r}_W)}. \tag{40}$$

In this paper, we assume the standard value of $\kappa(0) \approx 1.03$ [22,23]. Equation (40) then shows that \hat{s}_0^2 is inversely proportional to M_W^2 (strictly speaking $\Delta \hat{r}_W$ also depends on M_W via $\sin^2 \hat{\theta}_W(M_Z)$; however, since $\Delta \hat{r}_W \approx 0.06994 \ll 1$, we can safely ignore this dependence).

Equations (21) and (40) show the dependence of the SM value for Q_W on the physical mass M_W . Since the value of M_W is such that $\hat{s}_0^2 \approx 1/4$, the dependence is relatively weak for heavy atoms where N is large. Nevertheless, the extraordinary accuracy of APV experiments means that the measured weak charge could be sensitive to variations in the experimental value of M_W . It is also worth noting that the suppression due to the neutron is absent in the case of a proton, whose weak charge $Q_W(p) = -0.0719(45)$ [75] has an enhanced sensitivity to \hat{s}_0^2 . Thereby, renewed efforts on the atomic hydrogen APV experiment would be of great interest as an independent indirect probe of M_W mass.

Let us now consider the most recent result from the CDF II experiment at Tevatron [33], which found $M_W = 80,433.5 \pm 9.4 \text{ MeV}/c^2$, equivalent to a 7σ deviation from the SM model value of $M_W = 80,357 \pm 6 \text{ MeV}/c^2$. Ref. [33] also obtained a value of $M_Z = 91,192 \pm 7.5 \text{ MeV}/c^2$, which is consistent with the world average of $M_Z = 91,187 \pm 2.1 \text{ MeV}/c^2$. Plugging these values into Equations (21) and (40) and the formulae for radiative corrections [46], while assuming that all other parameters are unchanged, we find that the stand-alone CDF II result for M_W implies

$$Q_W^{\text{CDF II}}(^{133}\text{Cs}) = -73.11(1). \tag{41}$$

Our revised ^{133}Cs weak charge (41) corresponds to a shift of 0.16% or 8.5σ from the “old” SM value of $Q_W^{\text{SM}}(^{133}\text{Cs}) = -73.23(1)$. Our approach should be contrasted with global fits with $M_W = 80,433.5 \pm 9.4 \text{ MeV}/c^2$, which do not show an appreciable change in the value of $\sin^2 \hat{\theta}_W$, but rather slight variations in a wide array of EW parameters [34–37]. We believe that our approach makes the role of M_W more explicit and eliminates a potential bias.

Compared to the value extracted from Ref. [16], $Q_W^{2010} (^{133}\text{Cs}) = -73.16(29)_{\text{exp}}(20)_{\text{th}}$ and the result $Q_W^{2012} (^{133}\text{Cs}) = -72.58(29)_{\text{exp}}(32)_{\text{th}}$ extracted from Ref. [17] (the superscripts 2010 and 2012 denote the year of the corresponding publications), we have

$$Q_W^{2010} - Q_W^{\text{CDF II}} = -0.05(35), \tag{42}$$

$$Q_W^{2012} - Q_W^{\text{CDF II}} = 0.53(43), \tag{43}$$

where the uncertainties in Equations (42) and (43) were obtained by adding the corresponding theoretical and experimental errors and the uncertainty in Equation (41) in quadrature. From this, one observes that the result of Ref. [16] is 0.14σ smaller than the CDF II value while the result of Ref. [17] is 1.2σ larger. The comparison between these values is presented in Figure 1. Clearly, both results agree well with our revised SM value (41) within their respective error bars, while their average is in excellent agreement with (41).

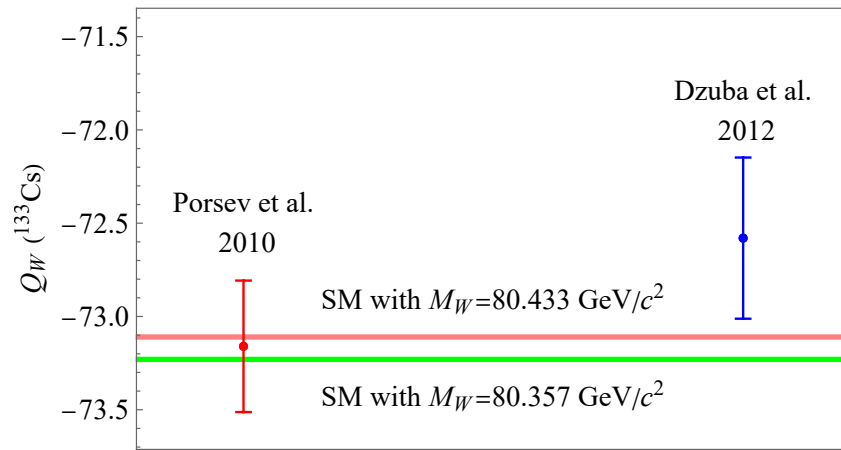


Figure 1. (Color online) Comparison between the ^{133}Cs nuclear weak charge as predicted by the Standard Model (SM) with the mass of the W boson being $M_W = 80.357 \text{ GeV}/c^2$ [82] (blue band), the SM with $M_W = 80.433 \text{ GeV}/c^2$ [33] (pink band), and ^{133}Cs APV experiment [1] with different calculations for the ^{133}Cs atomic structure factor (red and blue points).

Another substantial effect of the new value of M_W is on APV in atomic hydrogen due to the absence of the otherwise leading and M_W -independent neutron contribution to nuclear weak charge. Indeed, $M_W = 80,433.5 \pm 9.4 \text{ MeV}/c^2$ [33] implies a revised SM value for the proton weak charge

$$Q_W^{\text{CDFII}}(p) \approx 0.0730(21), \tag{44}$$

corresponding to a shift of 2.7% or 0.9σ away from the current SM prediction of $Q_W^{\text{SM}}(p) = 0.0711(2)$. It is also 1.5% or 0.22σ away from the nuclear physics measurement $Q_W(p) = 0.0719(45)$ [75]. A 1% measurement of a proton weak charge in APV experiments with hydrogen [107,108] may provide further evidence for or against the new CDF II result.

Using the new value for Q_W^{SM} (41), we can derive new constraints for the parameters of a new Z' boson appearing in Equation (23) as

$$\left(\frac{f_{AV}^{eq}}{M_{Z'}^2}\right)^{2010} = (5.2 \pm 3.6) \times 10^{-9} \text{ GeV}^{-2}, \tag{45}$$

$$\left(\frac{f_{AV}^{eq}}{M_{Z'}^2}\right)^{2012} = (-5.5 \pm 4.5) \times 10^{-9} \text{ GeV}^{-2}, \tag{46}$$

where, again, the superscript 2010 corresponds to Ref. [16], and the superscript 2012 corresponds to Ref. [17]. If we assume that the new Z' has the same couplings as Z , then by using Equation (25) and the value Q_W^{2012} , which results in a positive pull away from the SM, we obtain a direct constraint on $M_{Z'}$ as

$$M_{Z'} \geq 1.1 \text{ TeV}/c^2, \tag{47}$$

which is comparable to limits set by other electroweak precision data [109,110], interference effects at LEP-II [111], and the Tevatron [112].

Similarly, by using Equation (34), we can obtain constraints on the oblique parameter S of new vacuum polarization effects as

$$S^{2010} = 0.06(44), \tag{48}$$

$$S^{2012} = -0.66(54). \tag{49}$$

Finally, by using Equation (39), we derive updated constraints on the kinetic and mass mixing parameters of a dark Z_d boson as

$$\left[\delta^2 \left(1 - 1.28 \frac{\epsilon}{\epsilon_Z} \right) \right]^{2010} = 0.00684(3), \tag{50}$$

$$\left[\delta^2 \left(1 - 1.28 \frac{\epsilon}{\epsilon_Z} \right) \right]^{2012} = -0.00725(4). \tag{51}$$

4. Discussions

We have demonstrated how the recent measurement of the W boson mass [33] meaningfully affects the interpretation of APV experiments. More specifically, the new M_W boson mass implies a 0.16% shift in the SM prediction for the ^{133}Cs weak charge and a 2.7% shift in the prediction for the proton weak charge. We find that the new value for the ^{133}Cs nuclear weak charge reconciles the tension between the two most recent results for $Q_W(^{133}\text{Cs})$ extracted from the same experiment [1] but with different methods [16,17] of computing the atomic structure factor k_{PV} .

This reconciliation does not, however, signify an end to the story of APV. In fact, the disagreement between the two results [16,17], in particular the opposite signs of their estimates for the so-called core contribution, remains unexplained. Furthermore, since the uncertainties in these two results overlap one another and the new SM prediction (41) (see Figure 1), they provide little evidence for or against the new measurement of the new M_W boson mass. Such a confirmation or refutation may be possible, however, if the error bars in Figure 1 are reduced by half, i.e., to the level of $\lesssim 0.2\%$. In this sense, our result for ^{133}Cs provides further motivation for reducing the uncertainty in atomic calculations for APV [21]. It is worth mentioning that new measurements of electric dipole transition amplitudes in ^{133}Cs have recently been carried out at the level of $0.1\sim 0.2\%$ uncertainty [113–115]. These results serve as useful standards for gauging the accuracy of theoretical atomic calculations. Similarly, our results for the proton weak charge motivate next-generation APV experiments in hydrogen.

An alternative APV approach is the measurements of APV in a chain of isotopes, which forgoes the evaluation of atomic structure factors k_{PV} altogether. Such measurements yield ratios of weak charges, Q_W/Q'_W , of two nuclei with a fixed number of protons Z but differing number of neutrons (N and $N' = N + \Delta N$), see, e.g., Ref. [62]. In the isotopic-chain measurements, the sensitivity to M_W (through \hat{s}_0^2) can be expressed as

$$\frac{Q_W/N}{Q'_W/N'} \approx 1 - \frac{\Delta N}{N} \frac{Z}{N} \left(1 - 4\hat{s}_0^2 \right), \tag{52}$$

while in a single-isotope measurement, the relevant quantity is

$$\frac{Q_W}{-N} = 1 - \frac{Z}{N} \left(1 - 4\hat{s}_0^2 \right). \tag{53}$$

Comparing the two expressions, we see that in the isotopic-chain measurements, there is an extra suppression factor of $\Delta N/N$, which is $\ll 1$ for heavy nuclei of practical interest. Thereby, single-isotope measurements are more sensitive to varying M_W than the isotopic-chain experiments.

Throughout this paper, we have focused on how the new M_W measurement affects the SM prediction for the nuclear weak charges and thus limits new physics by changing the value of \hat{s}_0^2 . Evidence for beyond-SM contributions may also be constrained by direct low-energy precision measurements of the weak mixing angles themselves. Indeed, significant improvement in the short term is likely to come from PV polarized-electron scattering asymmetries at MESA [116] and Jefferson Lab [117] rather than from APV. Nevertheless, as noted above, new APV experiments and theoretical calculations at the level of 0.2% uncertainty will have meaningful long-term contributions to testing the SM at low energies. In

Figure 2, we plot the running of $\sin^2 \hat{\theta}_W$ with the W boson mass $M_W = 80.357 \text{ GeV}/c^2$ [82] and $M_W = 80.433 \text{ GeV}/c^2$ [33]. The change in M_W induces a downward 7.5σ shift in $\sin^2 \hat{\theta}_W$ across the energy scale up to 1 TeV. It may be observed that the blue curve, corresponding to $M_W = 80.357 \text{ GeV}/c^2$, gives a better fit to experimental measurements at the Z -pole, while the red curve, corresponding to $M_W = 80.433 \text{ GeV}/c^2$, gives a somewhat better fit to low-energy measurements. We reemphasize that this result is obtained by considering the new CDF-II value for $M_W = 80,433.5 \pm 9.4 \text{ MeV}/c^2$ while keeping all other SM parameters fixed. Global fits that include the new value for M_W do not show an appreciable change in the value of $\sin^2 \hat{\theta}_W$, but rather slight variations in a wide array of EW parameters [34–37]. We believe that our approach makes the role of M_W more explicit and eliminates a potential bias.

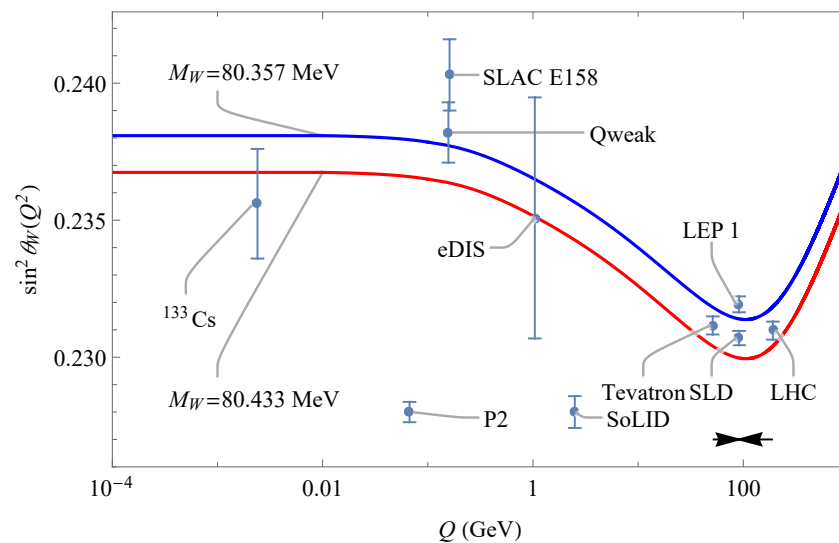


Figure 2. (Color online) Running of $\sin^2 \hat{\theta}_W$ predicted by the Standard Model (SM) with the mass of the W boson being $M_W = 80.357 \text{ GeV}/c^2$ [82] (blue line) and the SM with the new value $M_W = 80.433 \text{ GeV}/c^2$ [33] (red line). Results of several low-energy parity-violating lepton scattering experiments, as well as Z -pole measurements are also presented. The points P2 and SoLID are projected values from MESA’s P2 experiment [116] and Jefferson Lab’s SoLID experiment [117]. For clarity, the Tevatron and LHC results have been horizontally shifted.

5. Conclusions

In this paper, we showed that the stand-alone CDF-II value for the mass of the W -boson implies a 0.16% or 8.5σ shift in the Standard Model (SM) prediction of the ^{133}Cs weak charge. This shift, if exists, is potentially detectable by atomic parity violation (APV) experiments on ^{133}Cs with uncertainties $\lesssim 0.1\sim 0.2\%$. Effort to reduce the theoretical uncertainties of atomic calculation down to this level is in progress [21], whereas new APV experiments on ^{133}Cs are being planned [4,5]. Using the new SM prediction for the ^{133}Cs weak charge, we readjusted APV constraints on parameters of physics beyond the SM, such as the mass of a new Z' -boson, Equation (47), the oblique parameter of new vacuum polarization effects, Equation (48), and the kinetic and mass mixing parameters of a dark Z_d boson, Equation (50). We also showed that the stand-alone CDF-II value for the mass of the W -boson implies a 2.7% shift in the prediction for the proton weak charge, thus motivating new APV experiments in hydrogen.

Author Contributions: Formal analysis, H.B.T.T. and A.D.; Investigation, H.B.T.T.; Writing—original draft, H.B.T.T. and A.D.; Writing—review & editing, H.B.T.T. and A.D.; Supervision, A.D.; Project administration, A.D.; Funding acquisition, A.D. All authors have read and agreed to the published version of the manuscript.

Funding: This research was funded by the U.S. National Science Foundation grants PHY-1912465 and PHY-2207546, by the Sara Louise Hartman endowed professorship in Physics, and by the Center for Fundamental Physics at Northwestern University.

Data Availability Statement: Not applicable.

Acknowledgments: The authors thank Igor Samsonov and Xiaochao Zheng for helpful discussions. We thank Jens Erler for providing his code for computing radiative corrections.

Conflicts of Interest: The authors declare no conflict of interest.

References

1. Wood, C.S.; Bennett, S.C.; Cho, D.; Masterson, B.P.; Roberts, J.L.; Tanner, C.E.; Wieman, C.E. Measurement of Parity Nonconservation and an Anapole Moment in Cesium. *Science* **1997**, *275*, 1759–1763. [[CrossRef](#)] [[PubMed](#)]
2. Gomez, E.; Orozco, L.A.; Sprouse, G.D. Spectroscopy with trapped francium: Advances and perspectives for weak interaction studies. *Rep. Prog. Phys.* **2005**, *69*, 79–118. [[CrossRef](#)]
3. DeMille, D.; Cahn, S.B.; Murphree, D.; Rahmlow, D.A.; Kozlov, M.G. Using Molecules to Measure Nuclear Spin-Dependent Parity Violation. *Phys. Rev. Lett.* **2008**, *100*, 023003. [[CrossRef](#)]
4. Antypas, D.; Elliott, D.S. Measurement of a weak transition moment using two-pathway coherent control. *Phys. Rev. A* **2013**, *87*, 042505. [[CrossRef](#)]
5. Choi, J.; Sutherland, R.T.; Toh, G.; Damitz, A.; Elliott, D.S. Gain measurement scheme for precise determination of atomic parity violation through two-pathway coherent control. *arXiv* **2018**, arXiv:1808.00384.
6. Aubin, S.; Behr, J.; Collister, R.; Flambaum, V.; Gomez, E.; Gwinner, G.; Jackson, K.; Melconian, D.; Orozco, L.; Pearson, M.; et al. Atomic parity non-conservation: The francium anapole project of the FrPNC collaboration at TRIUMF. *Hyperfine Interact.* **2013**, *214*, 163–171. [[CrossRef](#)]
7. Portela, M.N.; van den Berg, J.; Bekker, H.; Böll, O.; Dijck, E.; Giri, G.; Hoekstra, S.; Jungmann, K.; Mohanty, A.; Onderwater, C.; et al. Towards a precise measurement of atomic parity violation in a single Ra⁺ ion. *Hyperfine Interact.* **2013**, *214*, 157–162. [[CrossRef](#)]
8. Altuntaş, E.; Ammon, J.; Cahn, S.B.; DeMille, D. Measuring nuclear-spin-dependent parity violation with molecules: Experimental methods and analysis of systematic errors. *Phys. Rev. A* **2018**, *97*, 042101. [[CrossRef](#)]
9. Altuntaş, E.; Ammon, J.; Cahn, S.B.; DeMille, D. Demonstration of a Sensitive Method to Measure Nuclear-Spin-Dependent Parity Violation. *Phys. Rev. Lett.* **2018**, *120*, 142501. [[CrossRef](#)]
10. Abe, K.; Abe, K.; Abe, T.; Adam, I.; Akimoto, H.; Aston, D.; Baird, K.G.; Baltay, C.; Band, H.R.; Barklow, T.L.; et al. High-Precision Measurement of the Left-Right Z Boson Cross-Section Asymmetry. *Phys. Rev. Lett.* **2000**, *84*, 5945–5949. [[CrossRef](#)]
11. LEP Collaboration; ALEPH Collaboration; DELPHI Collaboration; L3 Collaboration; OPAL Collaboration; LEP Electroweak Working Group. Precision Electroweak Measurements and Constraints on the Standard Model. *arXiv* **2010**, arXiv:1012.2367.
12. Dzuba, V.A.; Flambaum, V.V.; Silvestrov, P.G.; Sushkov, O.P. Relativistic many-body calculations in atoms and parity violation in caesium. *J. Phys. B* **1985**, *18*, 597–613. [[CrossRef](#)]
13. Dzuba, V.; Flambaum, V.; Sushkov, O. Summation of the high orders of perturbation theory for the parity nonconserving E1-amplitude of the 6s–7s transition in the caesium atom. *Phys. Lett. A* **1989**, *141*, 147–153. [[CrossRef](#)]
14. Blundell, S.A.; Johnson, W.R.; Sapirstein, J. High-accuracy calculation of the 6s_{1/2}→7s_{1/2} parity-nonconserving transition in atomic cesium and implications for the standard model. *Phys. Rev. Lett.* **1990**, *65*, 1411–1414. [[CrossRef](#)] [[PubMed](#)]
15. Blundell, S.A.; Sapirstein, J.; Johnson, W.R. High-accuracy calculation of parity nonconservation in cesium and implications for particle physics. *Phys. Rev. D* **1992**, *45*, 1602–1623. [[CrossRef](#)]
16. Porsev, S.G.; Beloy, K.; Derevianko, A. Precision determination of weak charge of ¹³³Cs from atomic parity violation. *Phys. Rev. D* **2010**, *82*, 036008. [[CrossRef](#)]
17. Dzuba, V.A.; Berengut, J.C.; Flambaum, V.V.; Roberts, B. Revisiting Parity Nonconservation in Cesium. *Phys. Rev. Lett.* **2012**, *109*, 203003. [[CrossRef](#)]
18. Sahoo, B.K.; Das, B.P.; Spiesberger, H. New physics constraints from atomic parity violation in ¹³³Cs. *Phys. Rev. D* **2021**, *103*, L111303. [[CrossRef](#)]
19. Roberts, B.M.; Ginges, J.S.M. Comment on “New physics constraints from atomic parity violation in ¹³³Cs”. *Phys. Rev. D* **2022**, *105*, 018301. [[CrossRef](#)]
20. Sahoo, B.K.; Das, B.P.; Spiesberger, H. Reply to “Comment on ‘New physics constraints from atomic parity violation in ¹³³Cs’”. *Phys. Rev. D* **2022**, *105*, 018302. [[CrossRef](#)]
21. Tran Tan, H.B.; Xiao, D.; Derevianko, A. Parity-mixed coupled-cluster formalism for computing parity-violating amplitudes. *Phys. Rev. A* **2022**, *105*, 022803. [[CrossRef](#)]
22. Marciano, W.J.; Sirlin, A. Radiative corrections to atomic parity violation. *Phys. Rev. D* **1983**, *27*, 552–556. [[CrossRef](#)]
23. Marciano, W.J.; Sirlin, A. Some general properties of the O(α) corrections to parity violation in atoms. *Phys. Rev. D* **1984**, *29*, 75–88. [[CrossRef](#)]

24. Czarnecki, A.; Marciano, W.J. Electroweak radiative corrections to polarized Møller scattering asymmetries. *Phys. Rev. D* **1996**, *53*, 1066–1072. [[CrossRef](#)] [[PubMed](#)]
25. Erler, J.; Kurylov, A.; Ramsey-Musolf, M.J. Weak charge of the proton and new physics. *Phys. Rev. D* **2003**, *68*, 016006. [[CrossRef](#)]
26. Marciano, W.J.; Rosner, J.L. Atomic parity violation as a probe of new physics. *Phys. Rev. Lett.* **1990**, *65*, 2963–2966; Erratum in *Phys. Rev. Lett.* **1992**, *68*, 898–898 [[CrossRef](#)]
27. Porsev, S.G.; Beloy, K.; Derevianko, A. Precision Determination of Electroweak Coupling from Atomic Parity Violation and Implications for Particle Physics. *Phys. Rev. Lett.* **2009**, *102*, 181601. [[CrossRef](#)]
28. Peskin, M.E.; Takeuchi, T. New constraint on a strongly interacting Higgs sector. *Phys. Rev. Lett.* **1990**, *65*, 964–967. [[CrossRef](#)]
29. Davoudiasl, H.; Lee, H.S.; Marciano, W.J. Muon Anomaly and Dark Parity Violation. *Phys. Rev. Lett.* **2012**, *109*, 031802. [[CrossRef](#)]
30. Davoudiasl, H.; Lee, H.S.; Marciano, W.J. “Dark” Z implications for parity violation, rare meson decays, and Higgs physics. *Phys. Rev. D* **2012**, *85*, 115019. [[CrossRef](#)]
31. Andreas, S. Update on hidden sectors with dark forces and dark matter. *arXiv* **2012**, arXiv:1211.5160.
32. Derevianko, A. Detecting dark-matter waves with a network of precision-measurement tools. *Phys. Rev. A* **2018**, *97*, 042506. [[CrossRef](#)]
33. CDF Collaboration; Aaltonen, T.; Amerio, S.; Amidei, D.; Anastassov, A.; Annovi, A.; Antos, J.; Apollinari, G.; Appel, J.A.; Arisawa, T.; et al. High-precision measurement of the W boson mass with the CDF II detector. *Science* **2022**, *376*, 170–176. [[CrossRef](#)] [[PubMed](#)]
34. Lu, C.T.; Wu, L.; Wu, Y.; Zhu, B. Electroweak Precision Fit and New Physics in light of W Boson Mass. *arXiv* **2022**, arXiv:2204.03796.
35. Fan, J.; Li, L.; Liu, T.; Lyu, K.F. W-Boson Mass, Electroweak Precision Tests and SMEFT. *arXiv* **2022**, arXiv:2204.04805.
36. de Blas, J.; Pierini, M.; Reina, L.; Silvestrini, L. Impact of the recent measurements of the top-quark and W-boson masses on electroweak precision fits. *arXiv* **2022**, arXiv:2204.04204.
37. Asadi, P.; Cesarotti, C.; Fraser, K.; Homiller, S.; Parikh, A. Oblique Lessons from the W Mass Measurement at CDF II. *arXiv* **2022**, arXiv:2204.05283.
38. Bhaskar, A.; Madathil, A.A.; Mandal, T.; Mitra, S. Combined explanation of W-mass, muon $g - 2$, $R_{K^{(*)}}$ and $R_{D^{(*)}}$ anomalies in a singlet-triplet scalar leptoquark model. *arXiv* **2022**, arXiv:2204.09031.
39. Heckman, J.J. Extra W-Boson Mass from a D3-Brane. *arXiv* **2022**, arXiv:2204.05302.
40. Athron, P.; Bach, M.; Jacob, D.H.; Kotlarski, W.; Stöckinger, D.; Voigt, A. Precise calculation of the W boson pole mass beyond the Standard Model with FlexibleSUSY. *arXiv* **2022**, arXiv:2204.05285.
41. Athron, P.; Fowlie, A.; Lu, C.T.; Wu, L.; Wu, Y.; Zhu, B. The W boson Mass and Muon $g - 2$: Hadronic Uncertainties or New Physics? *arXiv* **2022**, arXiv:2204.03996.
42. Liu, X.; Guo, S.Y.; Zhu, B.; Li, Y. Unifying gravitational waves with W boson, FIMP dark matter, and Majorana Seesaw mechanism. *arXiv* **2022**, arXiv:2204.04834.
43. Addazi, A.; Marciano, A.; Pasechnik, R.; Yang, H. CDF II W-mass anomaly faces first-order electroweak phase transition. *arXiv* **2022**, arXiv:2204.10315.
44. Greiner, W.; Müller, B. *Gauge Theory of Weak Interactions*; Springer: Berlin/Heidelberg, Germany, 1996.
45. Schwartz, M.D. *Quantum Field Theory and the Standard Model*; Cambridge University Press: Cambridge, UK, 2014.
46. Erler, J.; Su, S. The weak neutral current. *Prog. Part. Nucl. Phys.* **2013**, *71*, 119–149. [[CrossRef](#)]
47. Kumar, K.; Mantry, S.; Marciano, W.; Souder, P. Low-Energy Measurements of the Weak Mixing Angle. *Annu. Rev. Nucl. Part. Sci.* **2013**, *63*, 237–267. [[CrossRef](#)]
48. The ALEPH Collaboration; The DELPHI Collaboration; The L3 Collaboration; The OPAL Collaboration; The SLD Collaboration; The LEP Electroweak Working Group; The SLD Electroweak and Heavy Flavour Groups. Precision electroweak measurements on the Z resonance. *Phys. Rep.* **2006**, *427*, 257–454. [[CrossRef](#)]
49. Webber, D.M.; Tishchenko, V.; Peng, Q.; Battu, S.; Carey, R.M.; Chitwood, D.B.; Crnkovic, J.; Debevec, P.T.; Dhamija, S.; Earle, W.; et al. Measurement of the Positive Muon Lifetime and Determination of the Fermi Constant to Part-per-Million Precision. *Phys. Rev. Lett.* **2011**, *106*, 041803. [[CrossRef](#)]
50. Aoyama, T.; Kinoshita, T.; Nio, M. Theory of the Anomalous Magnetic Moment of the Electron. *Atoms* **2019**, *7*, 28. [[CrossRef](#)]
51. Bouchendira, R.; Cladé, P.; Guellati-Khélifa, S.; Nez, F.; Biraben, F. New Determination of the Fine Structure Constant and Test of the Quantum Electrodynamics. *Phys. Rev. Lett.* **2011**, *106*, 080801. [[CrossRef](#)]
52. Parker, R.H.; Yu, C.; Zhong, W.; Estey, B.; Müller, H. Measurement of the fine-structure constant as a test of the Standard Model. *Science* **2018**, *360*, 191–195. [[CrossRef](#)] [[PubMed](#)]
53. Bouchiat, M.; Guena, J.; Hunter, L.; Pottier, L. Observation of a parity violation in cesium. *Phys. Lett. B* **1982**, *117*, 358–364. [[CrossRef](#)]
54. Guéna, J.; Chauvat, D.; Jacquier, P.; Jahier, E.; Lintz, M.; Sanguinetti, S.; Wasan, A.; Bouchiat, M.A.; Papoyan, A.V.; Sarkisyan, D. New Manifestation of Atomic Parity Violation in Cesium: A Chiral Optical Gain Induced by Linearly Polarized $6S-7S$ Excitation. *Phys. Rev. Lett.* **2003**, *90*, 143001. [[CrossRef](#)] [[PubMed](#)]
55. Guéna, J.; Lintz, M.; Bouchiat, M.A. Measurement of the parity violating $6S-7S$ transition amplitude in cesium achieved within 2×10^{-13} atomic-unit accuracy by stimulated-emission detection. *Phys. Rev. A* **2005**, *71*, 042108. [[CrossRef](#)]
56. Tsigutkin, K.; Dounas-Frazer, D.; Family, A.; Stalnaker, J.E.; Yashchuk, V.V.; Budker, D. Observation of a Large Atomic Parity Violation Effect in Ytterbium. *Phys. Rev. Lett.* **2009**, *103*, 071601. [[CrossRef](#)]

57. Macpherson, M.J.D.; Zetie, K.P.; Warrington, R.B.; Stacey, D.N.; Hoare, J.P. Precise measurement of parity nonconserving optical rotation at 876 nm in atomic bismuth. *Phys. Rev. Lett.* **1991**, *67*, 2784–2787. [[CrossRef](#)]
58. Meekhof, D.M.; Vetter, P.; Majumder, P.K.; Lamoreaux, S.K.; Fortson, E.N. High-precision measurement of parity nonconserving optical rotation in atomic lead. *Phys. Rev. Lett.* **1993**, *71*, 3442–3445. [[CrossRef](#)]
59. Phipp, S.J.; Edwards, N.H.; Baird, P.E.G.; Nakayama, S. A measurement of parity non-conserving optical rotation in atomic lead. *J. Phys. B* **1996**, *29*, 1861–1869. [[CrossRef](#)]
60. Vetter, P.A.; Meekhof, D.M.; Majumder, P.K.; Lamoreaux, S.K.; Fortson, E.N. Precise Test of Electroweak Theory from a New Measurement of Parity Nonconservation in Atomic Thallium. *Phys. Rev. Lett.* **1995**, *74*, 2658–2661. [[CrossRef](#)]
61. Edwards, N.H.; Phipp, S.J.; Baird, P.E.G.; Nakayama, S. Precise Measurement of Parity Nonconserving Optical Rotation in Atomic Thallium. *Phys. Rev. Lett.* **1995**, *74*, 2654–2657. [[CrossRef](#)] [[PubMed](#)]
62. Antypas, D.; Fabricant, A.; Stalnaker, J.E.; Tsigutkin, K.; Flambaum, V.; Budker, D. Isotopic variation of parity violation in atomic ytterbium. *Nat. Phys.* **2019**, *15*, 120–123. [[CrossRef](#)]
63. Allaby, J.V.; Amaldi, U.; Barbiellini, G.; Baubillier, M.; Bergsma, F.; Capone, A.; Flegel, W.; Grancagnolo, F.; Lanceri, L.; Metcalf, M.; et al. A precise determination of the electroweak mixing angle from semileptonic neutrino scattering. *Z. Phys. C* **1987**, *36*, 611–628.
64. Blondel, A.; Böckmann, P.; Burkhardt, H.; Dydak, F.; Grant, A.L.; Hagelberg, R.; Hughes, E.W.; Krasny, W.; Para, A.; Taureg, H.; et al. Electroweak parameters from a high statistics neutrino nucleon scattering experiment. *Z. Phys. C* **1990**, *45*, 361–379. [[CrossRef](#)]
65. Zeller, G.P.; McFarland, K.S.; Adams, T.; Alton, A.; Avvakumov, S.; De Barbaro, L.; De Barbaro, P.; Bernstein, R.H.; Bodek, A.; Bolton, T.; et al. Precise Determination of Electroweak Parameters in Neutrino-Nucleon Scattering. *Phys. Rev. Lett.* **2002**, *88*, 091802. [[CrossRef](#)] [[PubMed](#)]
66. Akimov, D.; Albert, J.B.; An, P.; Awe, C.; Barbeau, P.S.; Becker, B.; Belov, V.; Brown, A.; Bolozdynya, A.; Cabrera-Palmer, B.; et al. Observation of coherent elastic neutrino-nucleus scattering. *Science* **2017**, *357*, 1123–1126. [[CrossRef](#)] [[PubMed](#)]
67. Prescott, C.Y.; Atwood, W.B.; Cottrell, R.L.A.; DeStaeblcr, H.; Garwin, E.L.; Gonidec, A.; Miller, R.H.; Rochester, L.S.; Sato, T.; Sherden, D.J.; et al. Further measurements of parity non-conservation in inelastic electron scattering. *Phys. Lett. B* **1979**, *84*, 524–528. [[CrossRef](#)]
68. Wang, D.; Pan, K.; Subedi, R.; Deng, X.; Ahmed, Z.; Allada, K.; Aniol, K.A.; Armstrong, D.S.; Arrington, J.; Bellini, V.; et al. Measurement of parity violation in electron-quark scattering. *Nature* **2014**, *506*, 67.
69. Wang, D.; Pan, K.; Subedi, R.; Ahmed, Z.; Allada, K.; Aniol, K.A.; Armstrong, D.S.; Arrington, J.; Bellini, V.; Beminiwattha, R.; et al. Measurement of parity-violating asymmetry in electron-deuteron inelastic scattering. *Phys. Rev. C* **2015**, *91*, 045506. [[CrossRef](#)]
70. Hasty, R.; Hawthorne-Allen, A.M.; Averett, T.; Barkhuff, D.; Beck, D.H.; Beise, E.J.; Blake, A.; Breuer, H.; Carr, R.; Covrig, S.; et al. Strange Magnetism and the Anapole Structure of the Proton. *Science* **2000**, *290*, 2117–2119. [[CrossRef](#)]
71. Beise, E.; Pitt, M.; Spayde, D. The sample experiment and weak nucleon structure. *Prog. Part. Nucl. Phys.* **2005**, *54*, 289–350. [[CrossRef](#)]
72. Argento, A.; Benvenuti, A.C.; Bollini, D.; Camporesi, T.; Heiman, G.; Monari, L.; Navarra, F.L.; Bozzo, M.; Brun, R.; Gennow, H.; et al. Electroweak asymmetry in deep inelastic muon-nucleon scattering. *Phys. Lett. B* **1983**, *120*, 245–250. [[CrossRef](#)]
73. Heil, W.; Ahrens, J.; Andresen, H.G.; Bornheimer, A.; Conrath, D.; Dietz, K.J.; Gasteyer, W.; Gessinger, H.J.; Hartmann, W.; Jethwa, J.; et al. Improved limits on the weak, neutral, hadronic axial vector coupling constants from quasielastic scattering of polarized electrons. *Nucl. Phys. B* **1989**, *327*, 1–31. [[CrossRef](#)]
74. Souder, P.A.; Holmes, R.; Kim, D.H.; Kumar, K.S.; Schulze, M.E.; Isakovich, K.; Dodson, G.W.; Dow, K.W.; Farkhondeh, M.; Kowalski, S.; et al. Measurement of parity violation in the elastic scattering of polarized electrons from ^{12}C . *Phys. Rev. Lett.* **1990**, *65*, 694–697. [[CrossRef](#)] [[PubMed](#)]
75. Androic, D.; Armstrong, D.S.; Asaturyan, A.; Averett, T.; Balewski, J.; Bartlett, K.; Beaufait, J.; Beminiwattha, R.S.; Benesch, J.; Benmokhtar, F.; et al. Precision measurement of the weak charge of the proton. *Nature* **2018**, *557*, 207–211.
76. Aaltonen, T.; Abazov, V.M.; Abbott, B.; Acharya, B.S.; Adams, M.; Adams, T.; Agnew, J.P.; Alexeev, G.D.; Alkhazov, G.; Alton, A.; et al. Combination of CDF and D0 W -Boson mass measurements. *Phys. Rev. D* **2013**, *88*, 052018. [[CrossRef](#)]
77. The ALEPH Collaboration; The DELPHI Collaboration; The L3 Collaboration; The OPAL Collaboration; The LEP Electroweak Working Group. Electroweak measurements in electron–positron collisions at W -boson-pair energies at LEP. *Phys. Rep.* **2013**, *532*, 119–244. [[CrossRef](#)]
78. Aaboud, M.; Aad, G.; Abbott, B.; Abdallah, J.; Abidinov, O.; Abeloos, B.; Abidi, S.H.; AbouZeid, O.S.; Abraham, N.L.; Abramowicz, H.; et al. Measurement of the W -boson mass in pp collisions at $\sqrt{s} = 7$ TeV with the ATLAS detector. *Eur. Phys. J. C* **2018**, *78*, 110. [[CrossRef](#)]
79. Abe, K.; Abe, K.; Abe, T.; Adam, I.; Akimoto, H.; Aston, D.; Baird, K.G.; Baltay, C.; Band, H.R.; Barklow, T.L.; et al. Improved Direct Measurement of Leptonic Coupling Asymmetries with Polarized Z Bosons. *Phys. Rev. Lett.* **2001**, *86*, 1162–1166. [[CrossRef](#)] [[PubMed](#)]
80. Aaltonen, T.; Amerio, S.; Amidei, D.; Anastassov, A.; Annovi, A.; Antos, J.; Apollinari, G.; Appel, J.A.; Arisawa, T.; Artikov, A.; et al. Measurement of $\sin^2\theta_{\text{eff}}^{\text{lept}}$ using e^+e^- pairs from γ^*/Z bosons produced in $p\bar{p}$ collisions at a center-of-momentum energy of 1.96 TeV. *Phys. Rev. D* **2016**, *93*, 112016. [[CrossRef](#)]

81. Abazov, V.M.; Abbott, B.; Acharya, B.S.; Adams, M.; Adams, T.; Agnew, J.P.; Alexeev, G.D.; Alkhazov, G.; Alton, A.; Askew, A.; et al. Measurement of the Effective Weak Mixing Angle in $p\bar{p} \rightarrow Z/\gamma^* \rightarrow \ell^+\ell^-$ Events. *Phys. Rev. Lett.* **2018**, *120*, 241802. [[CrossRef](#)] [[PubMed](#)]
82. Zyla, P.A.; Barnett, R.M.; Beringer, J.; Dahl, O.; Dwyer, D.A.; Groom, D.E.; Lin, C.J.; Lugovsky, K.S.; Pianori, E.; Robinson, D.J.; et al. Review of Particle Physics. *Prog. Theor. Exp. Phys.* **2020**, *2020*, 083C01.
83. Milstein, A.I.; Sushkov, O.P.; Terekhov, I.S. Calculation of radiative corrections to the effect of parity nonconservation in heavy atoms. *Phys. Rev. A* **2003**, *67*, 062103. [[CrossRef](#)]
84. Robinett, R.W.; Rosner, J.L. Prospects for a second neutral vector boson at low mass in SO(10). *Phys. Rev. D* **1982**, *25*, 3036–3064. [[CrossRef](#)]
85. Leung, C.N.; Rosner, J.L. Addendum to “Prospects for a second neutral vector boson at low mass in SO(10)”. *Phys. Rev. D* **1984**, *29*, 2132–2134. [[CrossRef](#)]
86. Langacker, P.; Robinett, R.W.; Rosner, J.L. New heavy gauge bosons in pp and $p\bar{p}$ collisions. *Phys. Rev. D* **1984**, *30*, 1470–1487. [[CrossRef](#)]
87. Cohen, E.; Ellis, J.; Enqvist, K.; Nanopoulos, D. Experimental predictions from the superstring. *Phys. Lett. B* **1985**, *165*, 76–82. [[CrossRef](#)]
88. Witten, E. Symmetry breaking patterns in superstring models. *Nucl. Phys. B* **1985**, *258*, 75–100. [[CrossRef](#)]
89. Dine, M.; Kaplunovsky, V.; Mangano, M.; Nappi, C.; Seiberg, N. Superstring model building. *Nucl. Phys. B* **1985**, *259*, 549–571. [[CrossRef](#)]
90. Durkin, L.; Langacker, P. Neutral-current constraints on heavy Z bosons. *Phys. Lett. B* **1986**, *166*, 436–442. [[CrossRef](#)]
91. Barger, V.; Deshpande, N.G.; Whisnant, K. Phenomenological mass limits on extra Z of E_6 superstrings. *Phys. Rev. Lett.* **1986**, *56*, 30–33. [[CrossRef](#)]
92. Bouchiat, C.; Pickett, C. Parity violation in atomic cesium and alternatives to the standard model of electroweak interactions. *Phys. Lett. B* **1983**, *128*, 73–78. [[CrossRef](#)]
93. Bouchiat, C.; Fayet, P. Constraints on the parity-violating couplings of a new gauge boson. *Phys. Lett. B* **2005**, *608*, 87–94. [[CrossRef](#)]
94. Casalbuni, R.; De Curtis, S.; Dominici, D.; Gatto, R. Bounds on new physics from the new data on parity violation in atomic cesium. *Phys. Lett. B* **1999**, *460*, 135–140. [[CrossRef](#)]
95. Nilles, H. Supersymmetry, supergravity and particle physics. *Phys. Rep.* **1984**, *110*, 1–162. [[CrossRef](#)]
96. Susskind, L. Dynamics of spontaneous symmetry breaking in the Weinberg-Salam theory. *Phys. Rev. D* **1979**, *20*, 2619–2625. [[CrossRef](#)]
97. Veltman, M. Limit on mass differences in the Weinberg model. *Nucl. Phys. B* **1977**, *123*, 89–99. [[CrossRef](#)]
98. Rosner, J.L. Role of present and future atomic parity violation experiments in precision electroweak tests. *Phys. Rev. D* **2002**, *65*, 073026. [[CrossRef](#)]
99. Fayet, P. Light spin- $\frac{1}{2}$ or spin-0 dark matter particles. *Phys. Rev. D* **2004**, *70*, 023514. [[CrossRef](#)]
100. Finkbeiner, D.P.; Weiner, N. Exciting dark matter and the INTEGRAL/SPI 511 keV signal. *Phys. Rev. D* **2007**, *76*, 083519. [[CrossRef](#)]
101. Arkani-Hamed, N.; Finkbeiner, D.P.; Slatyer, T.R.; Weiner, N. A theory of dark matter. *Phys. Rev. D* **2009**, *79*, 015014. [[CrossRef](#)]
102. Adriani, O.; Barbarino, G.C.; Bazilevskaya, G.A.; Bellotti, R.; Boezio, M.; Bogomolov, E.A.; Bonechi, L.; Bonghi, M.; Bonvicini, V.; Bottai, S.; et al. An anomalous positron abundance in cosmic rays with energies 1.5–100 GeV. *Nature* **2009**, *458*, 607–609. [[CrossRef](#)] [[PubMed](#)]
103. Holdom, B. Two $U(1)$'s and e charge shifts. *Phys. Lett. B* **1986**, *166*, 196–198. [[CrossRef](#)]
104. Davoudiasl, H.; Lee, H.S.; Marciano, W.J. Low Q^2 weak mixing angle measurements and rare Higgs decays. *Phys. Rev. D* **2015**, *92*, 055005. [[CrossRef](#)]
105. Czarnecki, A.; Marciano, W.J. Parity violating asymmetries at future lepton colliders. *Int. J. Mod. Phys. A* **1998**, *13*, 2235–2244. [[CrossRef](#)]
106. Czarnecki, A.; Marciano, W.J. Polarized Moller scattering asymmetries. *Int. J. Mod. Phys. A* **2000**, *15*, 2365–2375. [[CrossRef](#)]
107. Dunford, R.W.; Holt, R.J. Parity violation in hydrogen revisited. *J. Phys. G* **2007**, *34*, 2099–2118. [[CrossRef](#)]
108. Rasor, C.; Yost, D.C. Laser-based measurement of parity violation in hydrogen. *Phys. Rev. A* **2020**, *102*, 032801. [[CrossRef](#)]
109. Erler, J.; Langacker, P.; Munir, S.; Rojas, E. Improved constraints on Z' bosons from electroweak precision data. *J. High Energy Phys.* **2009**, *2009*, 017. [[CrossRef](#)]
110. del Aguila, F.; de Blas, J.; Pérez-Victoria, M. Electroweak limits on general new vector bosons. *J. High Energy Phys.* **2010**, *2010*, 33. [[CrossRef](#)]
111. The LEP Collaboration; ALEPH Collaboration; DELPHI Collaboration; L3 Collaboration; OPAL Collaboration; The LEP Electroweak Working Group. A Combination of Preliminary Electroweak Measurements and Constraints on the Standard Model. *arXiv* **2004**, arXiv:hep-ex/0412015.
112. Jaffré, M. Search for high mass resonances in dilepton, dijet and diboson final states at the Tevatron. *arXiv* **2009**, arXiv:0909.2979.
113. Toh, G.; Damitz, A.; Glotzbach, N.; Quirk, J.; Stevenson, I.C.; Choi, J.; Safronova, M.S.; Elliott, D.S. Electric dipole matrix elements for the $6p^2P_J \rightarrow 7s^2S_{1/2}$ transition in atomic cesium. *Phys. Rev. A* **2019**, *99*, 032504. [[CrossRef](#)]

114. Damitz, A.; Toh, G.; Putney, E.; Tanner, C.E.; Elliott, D.S. Measurement of the radial matrix elements for the $6s^2S_{1/2} \rightarrow 7p^2P_J$ transitions in cesium. *Phys. Rev. A* **2019**, *99*, 062510. [[CrossRef](#)]
115. Toh, G.; Chalus, N.; Burgess, A.; Damitz, A.; Imany, P.; Leaird, D.E.; Weiner, A.M.; Tanner, C.E.; Elliott, D.S. Measurement of the lifetimes of the $7p^2P_{3/2}$ and $7p^2P_{1/2}$ states of atomic cesium. *Phys. Rev. A* **2019**, *100*, 052507. [[CrossRef](#)]
116. Becker, D.; Bucoveanu, R.; Grzesik, C.; Kempf, R.; Imai, K.; Molitor, M.; Tyukin, A.; Zimmermann, M.; Armstrong, D.; Aulenbacher, K.; et al. The P2 experiment. *Eur. Phys. J. A* **2018**, *54*, 208. [[CrossRef](#)]
117. Zheng, X.; Erler, J.; Liu, Q.; Spiesberger, H. Accessing weak neutral-current coupling g_{AA}^{eq} using positron and electron beams at Jefferson Lab. *Eur. Phys. J. A* **2021**, *57*, 173. [[CrossRef](#)]